

## CLINICAL RESEARCH

# Prevalence and Characterization of External Cervical Resorption Using Cone Beam Computed Tomography

Isadora Carneiro Pereira Machado, DDS, MS,\* Marília Oliveira Morais, DDS, PhD,<sup>†</sup>  
 Adriana Lustosa Pereira Bicalho, DDS, PhD,<sup>‡</sup>  
 Patrícia Helena Pereira Ferrari, DDS, PhD,<sup>§</sup> Juliano Martins Bueno, DDS, MS,\*<sup>†</sup> José Luiz Cintra Junqueira, DDS, PhD,\* and  
 Mariana Quirino Silveira Soares, DDS, PhD\*

## ABSTRACT

**Introduction:** The aim of this study was to assess the prevalence of external cervical resorption (ECR) and characterize the cases of ECR using cone beam computed tomography (CBCT). **Methods:** High-resolution CBCT scans of 6216 patients (2280 males and 3936 females), consecutively acquired during the period July 2021 to March 2022, were analyzed. Identified cases of ECR were characterized by 3 evaluators regarding lesion height, circumferential spread, portal of entry proximity to root canal, stage, location, and width. **Results:** In a total of 38 patients and 40 teeth, ECR cases demonstrated an incidence of 0.61%. The median age of the patients was 39 years. Prevalence of ERC was 0.78% among males and 0.50% among females. The most affected teeth were the maxillary incisors and canines. The most frequent characteristics of the lesion were: extension up to the cervical third (47.5%), more than 270° circumferential spread (42.55%), probable pulpal involvement (57.5%), progressive stage (65%), supracrestal (52.1%) and mesial (34.7%) localization of >1 mm in size (52.1%) portals of entry. Cases with greater longitudinal involvement also showed greater circumferential progression ( $P = .008$ ). There was no association between portal of entry location and bone crest or ECR reparative phase ( $P = .42$ ). Inter-rater agreement ranged from good to very good. No association between portal of entry and ECR progression was observed. **Conclusions:** ECR showed low prevalence in the Brazilian population, affecting mostly anterior maxillary teeth of patients within a wide age range. CBCT allowed characterization of ECR lesions with good interobserver agreement. (*J Endod* 2023; ■:1–9.)

## KEY WORDS

Cone-beam computed tomography; diagnosis; invasive cervical resorption; root resorption; three-dimensional classification

External cervical resorption (ECR) is a relatively uncommon, insidious condition that begins on the external root surface, and gradually replaces the mineralized tooth structure with granulomatous fibrovascular or fibro-osseous tissue<sup>1</sup>. These lesions are usually asymptomatic and eventually discovered through routine evaluation as imaging findings<sup>2</sup>. Identification and evaluation of this condition strongly depends on radiographic interpretation<sup>3</sup>.

It is well established in the literature that cone beam computed tomography (CBCT) has high diagnostic value for diagnosis and management of potentially treatable ECR lesions when compared to conventional radiographs<sup>4-6</sup>. The American Association of Endodontists/American Academy of Oral and Maxillofacial Radiology (AAE/AAOMR) already issued a joint statement reiterating the use of CBCT to evaluate and follow up cases of ECR. The European Society of Endodontology (ESE) also highlights the relevance of CBCT for the management of these lesions<sup>7,8</sup>.

Appearance of ECR on CBCT can vary and it is influenced by its evolution, consisting of 3 stages: initial, with local destruction/disruption of the normal periodontal ligament and cementum; progressive (resorptive), when asymmetric hypodensity is observed, and reparative (remodeling), when calcified

## SIGNIFICANCE

This manuscript describes the prevalence and relevant characteristics of ECR for its clinical diagnosis and treatment planning using CBCT.

From the \*Oral Radiology Division, São Leopoldo Mandic Research Institute, Campinas, São Paulo, Brazil; <sup>†</sup>Department of Oral Radiology, Centro Integrado de Radiodontologia CIRO, Goiânia, Goiás, Brazil; <sup>‡</sup>UNIFASAN, Goiânia, Goiás, Brazil; and <sup>§</sup>Private Practice, Santo André, São Paulo, Brazil

Ethics Approval: This study is in accordance with the Declaration of Helsinki and was approved by the local Ethical Committee.

Address requests for reprints to Mariana Quirino Silveira Soares, Division of Oral Radiology, Faculdade São Leopoldo Mandic, Instituto de Pesquisa São Leopoldo Mandic, R. Dr José Rocha Junqueira, Campinas 13.045-755, Brazil. E-mail address: [mariana.soares@slmandic.edu.br](mailto:mariana.soares@slmandic.edu.br)  
 0099-2399/\$ - see front matter

Copyright © 2023 American Association of Endodontists.  
<https://doi.org/10.1016/j.joen.2023.11.003>

tissue is deposited, giving a mottled or cloudy appearance with more hyperdense areas. Resorption and repair can occur simultaneously in different areas of the same lesion<sup>9</sup>. Stage of evolution by CT scan should be the first aspect to consider for treatment planning. Lesions in reparative stage should be monitored, and intervention is indicated in progressive stages<sup>10</sup>.

Other tomographic aspects also guide treatment planning. The portal of entry is the place, single or multiple, where the whole resorptive process started on the external root surface<sup>9</sup>. Considering that treatment should address the source to avoid recurrence, its location determines an internal or external approach, with or without endodontic treatment<sup>11,12</sup>.

According to the three-dimensional (3D) classification system introduced by Patel et al<sup>13</sup>, ECR evaluation is performed based on 3 parameters: height, circumferential spread, and proximity to root canal. Three-dimensional (3D) ECR characterization is achieved through the combination of the obtained values from each parameter. This system favors evaluation of the real extension of the resorptive process, since expansion occurs not only in coronal-apical direction, but also in lingual-buccal direction. When there is minimal healthy structure remaining, treatment success rates are low<sup>10</sup>.

After establishing the ECR stage, if the possibility of a watch-and-wait approach is excluded, accessibility should be assessed next. External approach should be considered in cases of treatable ECR which present larger, supracrestal portals of entry located on buccal or proximal surfaces. Conversely, in cases with smaller, subcrestal portals of entry located in the proximal or lingual surfaces, internal approach through endodontic access becomes the best option<sup>2,11,14</sup> (Supplemental Figure S1).

Case reports comprise most of the current literature on ECR<sup>12,15,16</sup>, and information regarding its prevalence is scarce<sup>17,18</sup>. Additionally, detailed CBCT image analysis impacts appropriate treatment planning, and is critical for treatment success<sup>12</sup>. This implies that preoperative CBCT diagnosis should be as accurate as possible. However, it can be influenced by factors such as exposure parameters, voxel configurations, detector sensitivity, reconstruction algorithms and, above all, the examiners' interpretation skills<sup>19,20</sup>.

Therefore, this research aimed to evaluate the prevalence of ECR, explore the characteristics to be observed in CBCT images, and assess radiologists' agreement regarding these features' analysis. A minor

objective was to evaluate the relationship between the location of the portal of entry and the stage of ECR.

## MATERIALS AND METHODS

### Data Collection

This cross-sectional, observational, retrospective study is reported following STROBE guidelines<sup>21</sup>, after approval by the Ethics Committee of São Leopoldo Mandic Institution (number 56291422.6.0000.5374), São Paulo, Brazil.

CBCT scans of 6216 patients, consecutively obtained between July 2021 and March 2022 from a private dental radiology center database, were analyzed. Patients were referred to the dental radiology service for various diagnostic purposes. All included images were acquired using a PreXion 3D Inc. CBCT scanner (San Mateo, CA, USA) configured to high resolution with an 0.100 mm<sup>3</sup> isotropic voxel, in a 50 mm height and 50 mm diameter field of view (FOV), 90 kVp tube voltage and 4 mA current during an exposure of 33.5 seconds (with 1024 exposures per acquisition).

Exclusion criteria were as follows: (1) teeth with endodontic treatment, (2) teeth with endodontic treatment and an intra-radicular retainer, (3) teeth with associated pathologies such as inflammatory periapical diseases, (4) unerupted teeth, (5) teeth in the FOV periphery, (6) CBCT images with a large number of artifacts that would make diagnosis impossible, (7) teeth with extensive restorations, and (8) teeth with suspicion of caries.

### Image Analysis

Before the evaluation, training was conducted by an experienced radiologist who presented the classifications used in the study to the evaluators. Examples of tomographic images that were not part of the main sample were shown, illustrating each of the classifications.

All images were analyzed by a single evaluator (specialist in dental radiology and imaging) for initial identification. ECR diagnosis was determined when, in the 3 orthogonal planes, a hypodense, poor-delimited image or a hyperdense, mottled, bone-like density image (reparative mineralized tissue) was observed starting from the cervical third of the tooth root, possibly extending to middle and apical thirds, with circumferential root spread, bypassing the root canal<sup>13</sup> (Figure 1). Portals of entry were identified as a region of destruction of tooth structure, located in the cervical third, connecting the resorptive process and the adjacent periodontal ligament (Figure 2). In

cases where the portal of entry was not identified or 2 or more portals of entry were visualized, additional evaluation was conducted by a fourth evaluator, a radiologist with 10 years of experience, to confirm the diagnosis.

After identification, cases were randomly and anonymously organized and later evaluated by 3 radiologists with experience of 5+ years, one of them also an endodontist. Images in DICOM format were analyzed in an environment with adequate lighting, using the same high-resolution monitor and the same OnDemand3D Technology software (Yuseong-gu, Daejeon, Republic of Korea), allowing free adjustment of brightness and contrast, and dynamic navigation of the images.

The following information was recorded and tabulated for each tooth with ECR (Figures 1-4):

1. Crestal position of the portal of entry: supracrestal or subcrestal;
2. Location of the portal of entry: mesial, distal, vestibular or lingual/palatal;
3. Size of the portal of entry:  $\leq 1$  mm,  $> 1$  mm;
4. Number of portals of entry;
5. Longitudinal spread: 1, 2, 3 or 4<sup>13</sup>;
6. Circumferential spread: A, B, C or D<sup>13</sup>;
7. Proximity to the root canal: d-confined to dentin, p-in communication with the pulp<sup>13</sup>;
8. Evolutionary stage of the lesion: progressive or reparative;
9. Patient age;
10. Gender of patient;
11. Affected tooth.

According to the 3D classification system introduced by Patel et al<sup>13</sup>, ECR evaluation was based on 3 parameters: height, circumferential spread, and proximity of the lesion to the root canal. The height of the lesion is scored as followed: (1) At cemento-enamel junction level or above the bone crest (supracrestal), (2) Below the bone crest (subcrestal), extending to the cervical third, (3) Extending to the middle third of the root, or (4) Extending to the apical third of the root. Circumference was classified according to their maximum spread: A) Less than 90°, B) Between 90° and 180°, C) Between 180° and 270°, and D) Greater than 270°. Proximity to the root canal was graded as follows: Confined to dentin (*d*), or with pulpal involvement (*p*). The value of each parameter was combined to describe ECR 3D characterization.

To standardize root length definition and determine longitudinal extent of ECR, we established a measurement from the

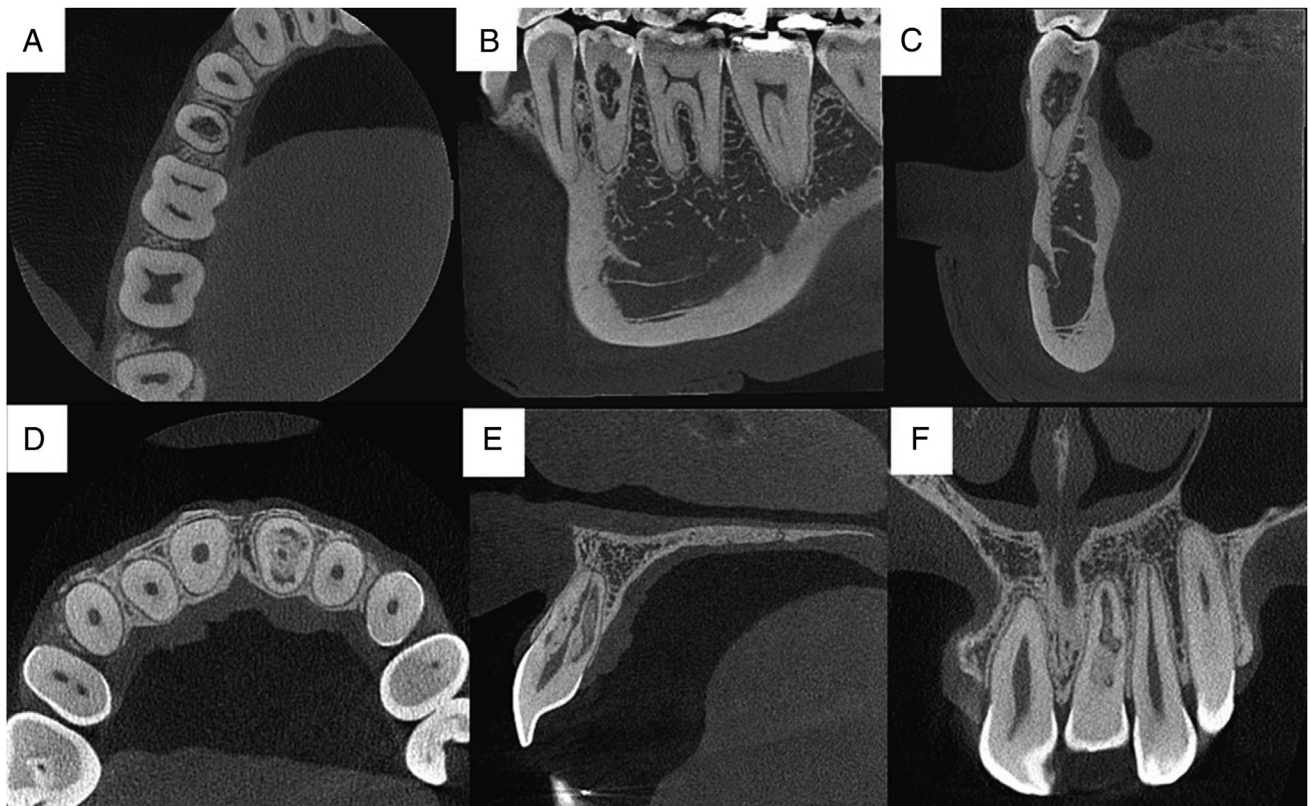


**FIGURE 1** – ECR stages: A, B, C- progressive stage on left mandibular second premolar; D, E, F: reparative stage on left maxillary lateral incisor.

cemento-enamel junction to the tooth apex; for circumferential spread, we drew 2 lines on the axial plane, dividing it into 4 quadrants. All images were reevaluated by the 3 examiners 15 days after the first evaluation under the same conditions.

### Statistical Analysis

To characterize the assessed variables, absolute (*n*) and relative (%) frequencies were used. Association between genders and the frequency of ECR and between the crestal position of the portal of entry and the stage of the lesion was evaluated using the Chi-square test. The significance level was set at  $P \leq .05$ . To verify the assessment error, Cohen's Kappa Coefficient for intraobserver agreement and percentages of inter- and intra-observer agreement were calculated. For inter-observers' concordance regarding assessed measures, Altman's proposed cut-off points (1991) were considered:  $\leq 0.20$  indicated weak agreement,  $0.21-0.40$  indicated reasonable or fair agreement,  $0.41-0.60$  indicated moderate agreement,  $0.61-0.80$  indicated good agreement,  $0.81-1.00$  indicated very good agreement<sup>22</sup>. Concordance between the 3 raters' ratings was assessed using Krippendorff's Alpha<sup>23</sup>.

Statistical analysis of the data was performed using the Statistical Package for the Social Sciences (SPSS)<sup>24</sup> program, version 29 for Windows (IBM Corp. Released, 2023).

## RESULTS

### Prevalence

This sample included a total of 6216 patients (2280 males and 3936 females), 38 of which exhibited ECR (40 teeth), resulting in a 0.61% prevalence. The patient's age ranged from 25 to 75 years, with a mean age of  $42.3 (\pm 11.9)$ ; median of 39 years: 28.9% were 25 to 34 years old, 34.2% were 35 to 44 years old, 23.7% were 45 to 54 years old, and 13.2% were 55 or older. Of the 38 patients, 20 (52.6%) were female and 18 (47.4%) were male. Prevalence of ECR was 0.78% among males and 0.50% among females with no significant difference between genders according to the Chi-square test ( $P = .08$ ). The most affected teeth were the maxillary central incisors (20%), maxillary canines (20%), and mandibular molars (7.5%) (Table 1).

### Tomographic Aspects

As for circumferential spread, according to Patel et al classification<sup>13</sup>, 40% of cases were classified as B ( $>90$  to  $\leq 180^\circ$ ), 17.5% as C

( $>180$  to  $\leq 270^\circ$ ) (Figure 3, and 42.5% as D ( $>270^\circ$ ); no cases were recorded as A ( $\leq 90^\circ$ ). The longitudinal extension was above the bone crest/cemento-enamel junction level (type 1) in 2.5% of the cases, below the bone crest/extending to the cervical third of the root (type 2) in 47.5%, extending to the mid-third of the root (type 3) in 30%, and extending to the apical third of the root (type 4) in 20%.

Regarding proximity to the root canal, dentin-confined lesions (*d*) were recorded in 42.5% of cases, and probable pulpal involvement (*p*) in 57.5%. The lesions' stage was progressive in 65% of cases and reparative in 30% (Table 2). In 2 cases (5%), both stages applied.

The portal of entry was identified in 67.5% (27 cases), with 2 or more portals of entry in 4 (10%) cases. No portal of entry was identified in 13 (32.5%) cases. Additional classification was performed only in cases where one portal of entry was observed (23 lesions): 39.1% demonstrated mesial localization, and 4.3% distal, 34.7% buccal, and 21.7% palatal/lingual localization. One (10%) of the 10 cases with subcrestal portal of entry was in the reparative stage, and 9 (90%) in the progressive stage.

The size of the portal of entry was less than 1 mm in 11 (47.8%) of the 23 cases with



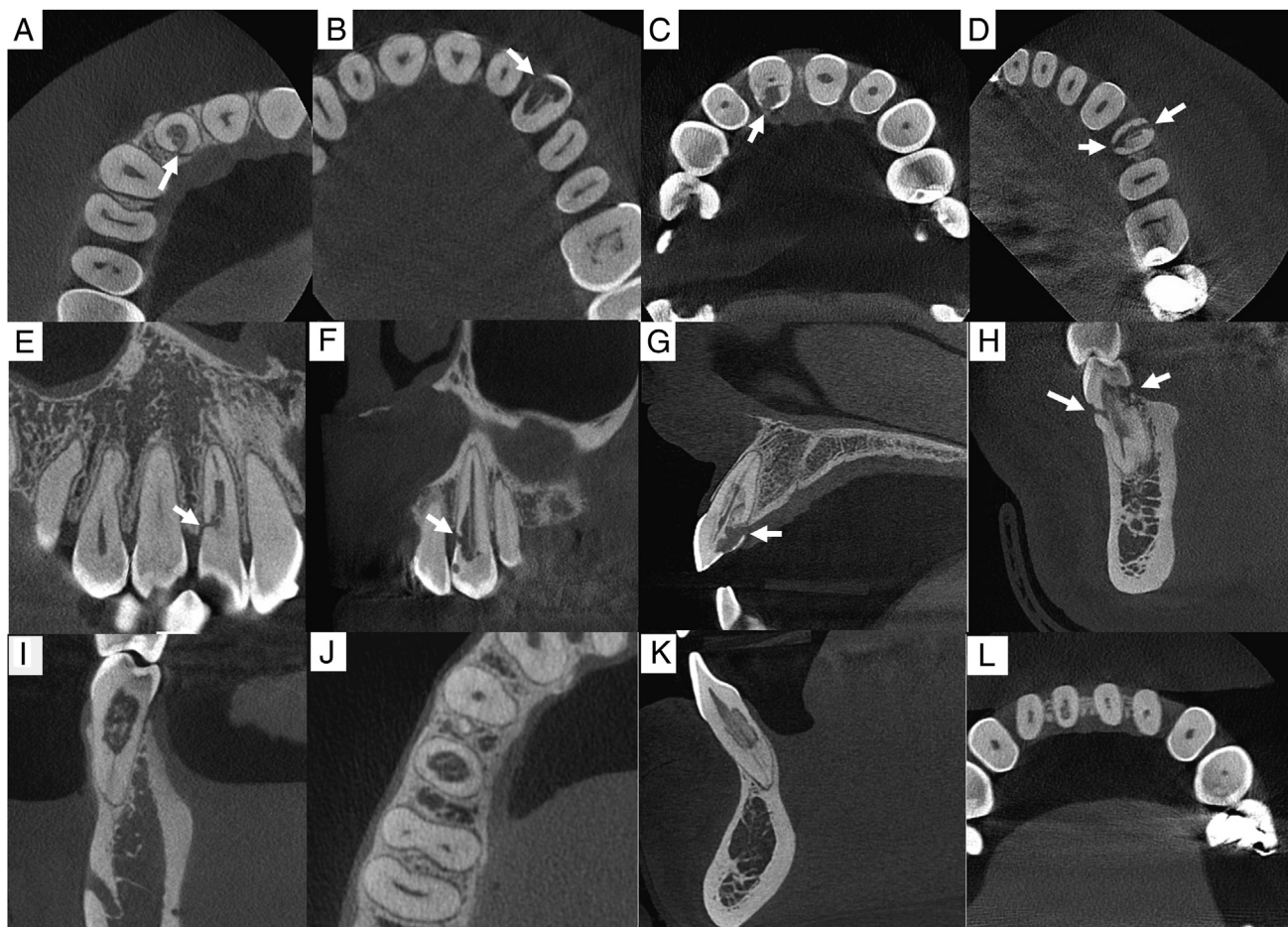


**FIGURE 2** – Portal of entry examples: *A, E*—subcrestal, distal,  $\leq 1$  mm (right maxillary central incisor); *B, F*—supracrestal, mesial,  $\leq 1$  mm (left maxillary canine); *C, G*—supracrestal, palatal,  $>1$  mm (right maxillary central incisor); *D, H*—two portals of entry: one being supracrestal, buccal and  $\leq 1$  mm, and the other being supracrestal, lingual and  $>1$  mm (left maxillary first premolar). Portal of entry unidentified: *I, J*—invasive cervical resorption in a progressive stage with; *K, L*—invasive cervical resorption in a reparative stage.

a portal of entry and greater than 1 mm in 12 (52.17%) cases. Supracrestal portal of entry was the most frequent (60.8% - 14 cases), and subcrestal was present in 9 (39.1%) cases (Table 2).

### Relationship Between Circumferential and Longitudinal Spread

The relationship between longitudinal and circumferential destruction was investigated using Fischer's exact test and showed statistically significant association ( $P < .05$ ). Cases with a greater degree of circumferential destruction also showed greater longitudinal extent (Tables 3 and 4).

### Relationship Between the Crestal Location of the Portal of Entry and the Stage of Lesion Evolution

Among the cases in which a portal of entry could be identified ( $n = 23$ ), 14 cases were

supracrestal. Of these, 9 (64.28%) were in the progressing stage, 3 (21.42%) in the reparative stage, and 2 (14.28%) showed identifiable signs of both stages concomitantly. Of the 9 cases with subcrestal portal of entry, 8 (88.9%) were in the progressive stage and only one case was in the reparative stage. No association was observed between the crestal position of the portal of entry and the stage of the lesion ( $P = .42$ ) (Tables 3 and 4). No portal of entry was identified in 13 (32.5%) cases. Of these, 53.8% and 46.15% were in reparative and progressive stage, respectively.

The results show concordance percentages greater than 70% among the 3 observers. Krippendorff Alpha values for the concordance agreement among the 3 observers indicated acceptable agreement (between 0.663 and 0.879). As for the intra-observer error analysis, agreement percentages higher than 77% and Kappa

Coefficient values between 0.651 and 1.000 were recorded (Table 5).

## DISCUSSION

The aim of this study was to document the prevalence and characterization of ECR lesions on high-resolution CBCT scans. To date, this study represents the largest population assessed on this topic, totaling 6216 CBCT scans with a 0.61% prevalence of ECR cases. Previous prevalence data on the current literature range from 0.02% to 2.3%<sup>17,25</sup>. A rate of 0.02% was found in a study comparing 222 patients with ECR with the total Australian population<sup>17</sup>, while the highest prevalence rate ever reported was 2.3% (98 teeth with ECR) on a retrospective case-control study based on a 10-year observation of patients of a university clinic in Vancouver, Canada<sup>25</sup>. In these previous studies, cases of ECR were diagnosed based on clinical and radiographic information in



**FIGURE 3** – ECR examples (*arrows*), according to Patel et al classification<sup>13</sup>: *A, D*- 2Bd (extending to the cervical third, 180° circumferential spread, confined to dentin (left maxillary first molar); *B, E*- 3Cd (extending to the middle third, 270° of circumferential spread, confined to dentin) (left mandibular first molar); *C, F*- 4Dd (extending into the apical third, 360° of circumferential progression, confined to dentin) (left maxillary lateral incisor).

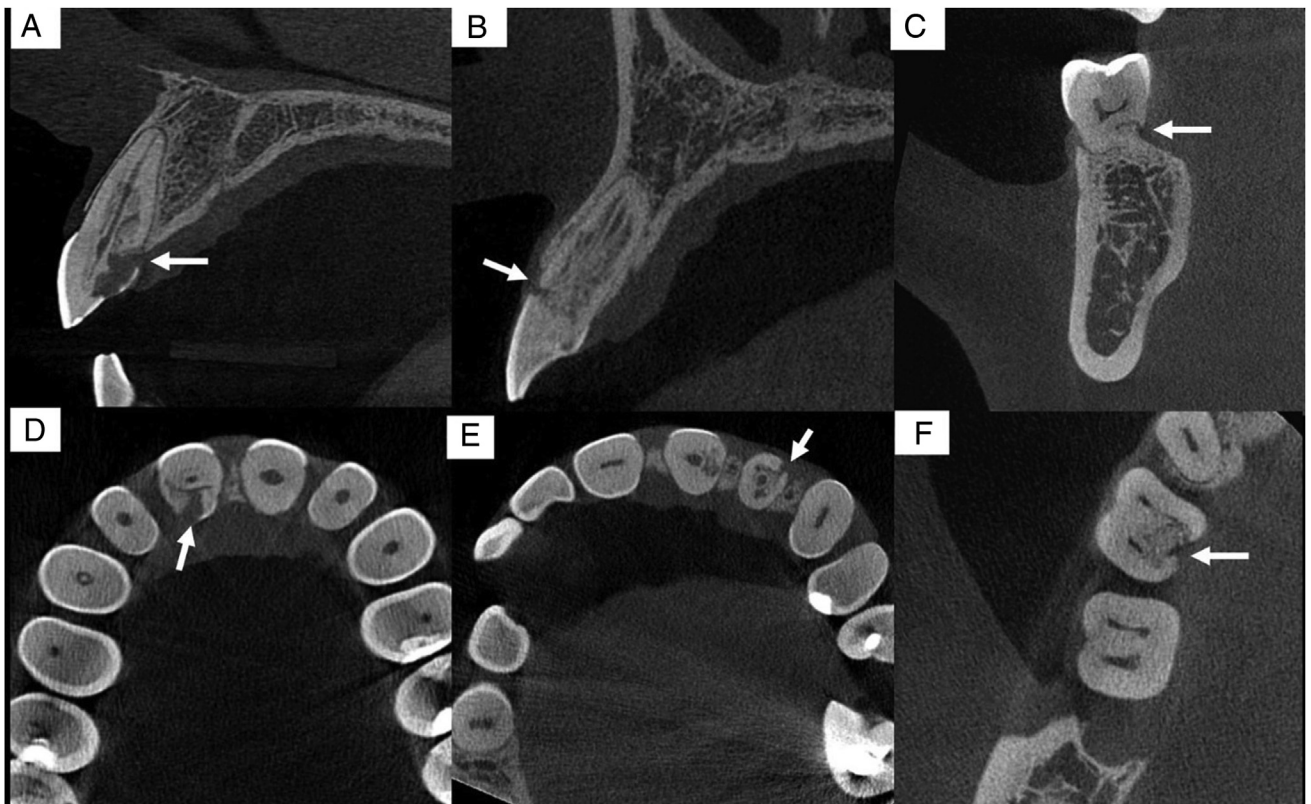


**FIGURE 4** – Unrepaired supracrestal port of entry examples (hypodense tissue, indicated by *arrows*), reparative stage: *A, D*: Case 1; *B, E*: Case 2; *C, F*: Case 3.



**TABLE 1** - Distribution According to Assessed Teeth ( $n = 40$ )

Assessed teeth group	n	%
Maxillary central incisors	8	20%
Maxillary lateral incisors	4	10%
Maxillary canines	8	20%
Maxillary premolars	4	10%
Maxillary molars	4	10%
Mandibular central incisors	2	5%
Mandibular canines	1	2.5%
Mandibular premolars	2	5%
Mandibular molars	7	17.5%

patients who were referred to dental clinics. The main purpose of these studies was to evaluate disease-related risk factors, so total sample size was not characterized. Diagnosis based on radiographic findings is considered limited because many lesions in early stages can be confused with caries<sup>16</sup>. A recent

retrospective Brazilian study of 1313 CBCT scans found a prevalence of 1.35%<sup>26</sup>.

Our findings agree with a preceding report, which concluded that ECR has a wide age distribution (18–81 years), with a mean age of 45.77 years<sup>27</sup>. However, the age range reported in this study was recorded at the moment of CBCT evaluation, and it's important to consider that it may not precisely reflect the period of lesion onset and development. In this study, prevalence of ECR was 0.78% among males and 0.50% among females with no significant difference between genders. This result differs from a recent study that showed higher prevalence in males<sup>26</sup>.

Unlike other resorption processes, the higher degree of complexity of ECR and the unusual imaging pattern of these lesions in CBCT make the evaluation challenging. Although agreement ranged from good to very good, lower Kappa values were observed when analyzing lesion stage, longitudinal

spread and pulpal involvement. Since it is a dynamic process, areas in both active resorption and repair can be simultaneously found<sup>9</sup>. As a result, there may be 2 imaging patterns in different sites of the same resorption, making it difficult to determine a single stage. In a study comparing CBCT, micro-CT, nano-CT, and histological sections, the authors concluded that CBCT images fail to identify reparative tissue formation<sup>28</sup>. This may explain the difference in agreement between examiners to determine lesion stage.

Concerning longitudinal spread assessment, the irregular, ill-defined propagation of the ECR in dental tissues<sup>3</sup> may have generated conflict about the end of the lesion. Considering that the alveolar bone crest is used as a reference to determine the longitudinal extent of the lesion, the 3D classification of Patel et al<sup>13</sup> is not clear about supracrestal ECR cases with some degree of bone resorption and substantial root involvement. Nevertheless, good agreement rates were obtained for this variable<sup>29</sup>. Also, understanding that the root is divided into cervical, middle, and apical thirds, with the cemento-enamel junction and the apex being fixed reference points, we still considered that we obtained good agreement rates for all variables.

Evaluation of longitudinal spread revealed that 19 cases (47.5%) were limited to the cervical root third; among these, more than half had already spread more than 90° and up to 180° circumferentially; of the 20 cases that extended to the middle or apical root third (50%), more than half had already advanced to more than 270° of root circumference. This finding indicates that resorption progresses proportionally in the coronal apical direction, and lingual/palatal vestibule, reinforcing the need for evaluation of the circumferential spread proposed earlier<sup>13</sup>.

Description of the longitudinal and circumferential extensions allows standardized classification of the remaining healthy root structure. Therefore, it can be useful to treatment planning<sup>13</sup>. When the ECR extends to the root's apical third or affects large circumferential dimensions (Patel's 4D classification<sup>13</sup>), it becomes difficult to remove all the granulation tissue without losing a large amount of healthy tooth tissue, compromising the periodontal stability of the tooth and leaving it susceptible to fracture. Hence, the best solution is immediate extraction, or observation until some symptom occurs<sup>29</sup>. A clinical study of 101 teeth affected by various degrees of ECR, with follow-up from 3 to 12 years, showed a 100% success rate of treatment in class 1 and 2 resorptions, 77.8% in class 3 lesions, and 12.5% in class 4 lesions.

**TABLE 2** - Characterization of the Assessed Variables - Circumferential Spread, Longitudinal Spread, Proximity to the Root Canal, Lesion Stage, Port of Entry Characteristics (Number, Localization, Size and Position) ( $n = 40$ )

Variables	N	%
Circumferential spread		
≤ 90°	0	0.0%
>90° - ≤ 180°	16	40.0%
>180° - ≤ 270°	7	17.5%
>270°	17	42.5%
Longitudinal spread		
Supracrestal/cemento-enamel junction	1	2.5%
Subcrestal/Extension towards the cervical third of the root	19	47.5%
Extension towards the mid-third of the root	12	30.0%
Extension towards the apical third of the root	8	20.0%
Root canal proximity		
Confined to dentin	17	42.5%
Probable pulpar involvement	23	57.5%
Stage		
Progressive	26	65.0%
Reparative	12	30.0%
Progressive and Reparative	2	5.0%
Number of portal of entry ( $n = 40$ )		
0	13	32.5%
1	23	57.5%
2	2	5.0%
3	1	2.5%
4	1	2.5%
Localization of portal of entry* ( $n = 23$ cases with a single-entry port)		
Mesial	9	39.1%
Distal	1	4.3%
Buccal	8	34.7%
Palatal/Lingual	5	21.7%
Size of portal of entry ( $n = 23$ cases with a single portal of entry)		
< 1 mm	11	47.8%
> 1 mm	12	52.2%
Crestal position of portal of entry ( $n = 23$ cases with a single portal of entry)		
Supracrestal	14	60.8%
Subcrestal	9	39.1%

\*Possibility of more than one location per case.

**TABLE 3** - Circumferential Spread According to Longitudinal Spread

Longitudinal spread	Circumferential				Total	P Value
	≤90°	>90° - ≤180°	>180° - ≤270°	270°		
Supracrestal/cemento-enamel junction	0 (0.0%)	1 (100.0%)	0 (0.0%)	0 (0.0%)	1 (100.0%)	.008
Subcrestal/Extension towards the cervical third of the root	0 (0.0%)	11 (57.9%)	5 (26.3%)	3 (15.8%)	19 (100.0%)	
Extension towards the mid-third of the root	0 (0.0%)	3 (25.0%)	2 (16.7%)	7 (58.3%)	12 (100.0%)	
Extension towards the apical third of the root	0 (0.0%)	1 (12.5%)	0 (0.0%)	7 (87.5%)	8 (100.0%)	

As expected, smaller lesions offer the most favorable long-term outcome<sup>10</sup>.

The Pericanal Resorption Resistant Sheet (PRRS) is a protective layer that surrounds the pulp tissue and prevents the resorption process from coming into contact with the pulp. Its presence is pointed out as a characteristic of ECR<sup>1</sup>. In this investigation, probable pulpal involvement was observed in 57.5% of cases. This unexpected finding may have happened because, even in presence of the PRRS layer, some small points of communication with the pulp were identified in the CBCT. This fact has already been a finding in 2 studies<sup>9,28</sup>, which detected occasional histological ruptures of this protective layer, especially towards coronal thirds, where it is thinner. Thus, the visualization of PRRS does not ensure absence of contact with pulp tissues, making CBCT dynamic evaluation essential to detect these small points of communication. This reinforces the need to use CBCT at high resolution parameters.

The 3 observers could not identify the portal of entry in 32.5% of the cases. This finding cannot be compared with other studies, because to our knowledge, there are no previous studies with this information. In 53.8 % of the cases without identified portal of entry, ECR lesions were in the reparative stage. In these cases, deposition of reparative bone tissue through the portal of entry (which is the starting point for the destructive process as well as the area where the deposition of mineralized tissue begins) leads alveolar bone and dentin fusion, making identification of those tissues difficult<sup>25</sup>. In the remaining cases

(46.15%), which were in a progressive stage, we believe that the reduced dimensions of the portal of entry may make obscure visualization, even with high resolution images. Finally, cases with advanced resorptive processes in direct contact with the dentin margins at several areas can also hinder portal of entry identification.

During evaluation, the examiners observed 3 reparative ECR cases where the portal of entry was located in a supracrestal position. However, despite the reparative stage classification of those cases, images showed that this defect was filled with hypodense (inflammatory) tissue. It was hypothesized that supracrestal portals of entry have fewer chances of remineralization, since local bacteria present in the crevicular sulcus influence clastic cell activity.

The 3D classification by Patel et al (2018b)<sup>13</sup> has been shown to be efficiently used in communication between dental surgeons and radiologists, but we must emphasize that it does not include data on lesion stage, and location and size of the portal of entry, which are fundamental aspects to assess during treatment planning. The limitations of this study should be acknowledged. First, the absence of clinical information that could aid in ECR diagnosis should be noted. Second, a limited field of view was evaluated for each patient. While this was necessary to ensure the appropriate image acquisition protocol with sufficient resolution for ECR diagnosis<sup>30-33</sup>, this methodological choice may affect the number of teeth assessed and the prevalence data

observed in this investigation. Hence, it was not possible to investigate the prevalence of ERC among each teeth group. Finally, the initial screening of images was performed by a single examiner. Thus, future studies relating clinical information to CBCT findings should also be encouraged in order to guide the treatment of ECR.

## CONCLUSIONS

In conclusion, ECR showed low prevalence, no significant gender predilection, and a wide age range. The portal of entry should be characterized in descriptive reports highlighting size and location in relation to the bone crest, as a way to assist the dentist's image interpretation, and consequent therapeutic decisions about internal or external approaches. Although no association was observed between the portal of entry and the lesion stage, our results suggest that supracrestal portals of entry may manifest with areas in the progressive stage, even if the lesion is predominantly reparative.

Since ECR is a dynamic process, it is possible to observe both progressive and reparative processes in some ECR cases. Priority should be given to determining the predominant stage in order to establish the appropriate therapeutic approach. Through dynamic navigation, intercommunication of the pulp and the resorptive process was observed, even with the presence of Pericanal Resorption Resistant Sheet. Difficulties in identification of ECR using CBCT are to be expected, especially in reparative stages.

**TABLE 4** - Lesion Stage According to the Portal of Entry

Portal of entry	Lesion stage			Total	P Value
	Progressive	Reparative	Progressive and reparative		
Supracrestal	9 (64.28%)	3 (21.42%)	2 (14.28%)	14 (100%)	.42
Subcrestal	8 (88.8%)	1 (11.1%)	0 (0.0%)	9 (100%)	

TABLE 5 - Inter-Examiner Agreement

Variables	Intra-observer		Principal observer vs. Observer 1 vs. Observer 2	
	C. Kappa	Concordance percentage (%)	Krippendorff Alpha	Concordance percentage (%)
Circumferential spread	0.651	77.5%	0.746	75.0%
Root canal proximity	0.754	87.5%	0.698	77.5%
Stage	0.826	92.5%	0.694	70.0%
Longitudinal spread	0.693	80.0%	0.663	62.5%
Portal of entry number	0.873	92.5%	0.710	75.0%
Portal of entry size	1.000	100.0%	0.758	78.9%
Portal of entry crest position	0.870	94.4%	0.758	78.9%
Portal of entry localization				
Mesial	0.667	83.3%	0.879	94.7%
Distal	1.000	100.0%	0.787	94.7%
Buccal	0.667	83.3%	0.767	89.5%
Palatal/Lingual	0.852	94.4%	0.808	89.5%

## CREDIT AUTHORSHIP CONTRIBUTION STATEMENT

**Isadora Carneiro Pereira Machado:** Conceptualization, Data curation, Formal analysis, Writing – original draft. **Marília Oliveira Morais:** Data curation, Writing – review & editing. **Adriana Lustosa Pereira Bicalho:** Data curation, Writing – review & editing. **Patricia Helena Pereira Ferrari:** Formal analysis, Writing – review & editing. **Juliano Martins Bueno:** Data curation,

Formal analysis, Writing – review & editing.

**José Luiz Cintra Junqueira:** Conceptualization, Supervision, Writing – review & editing. **Mariana Quirino Silveira Soares:** Conceptualization, Formal analysis, Supervision, Writing – review & editing.

*de Radiodontologia) for granting access to the tomographic images used in this study.*

*The authors deny any conflicts of interest related to this study.*

## ACKNOWLEDGMENTS

*The authors would like to express their gratitude to CIRO Institute (Centro Integrado*

## SUPPLEMENTARY MATERIAL

*Supplementary material associated with this article can be found in the online version at [www.jendodon.com \(https://doi.org/10.1016/j.joen.2023.11.003\)](https://doi.org/10.1016/j.joen.2023.11.003).*

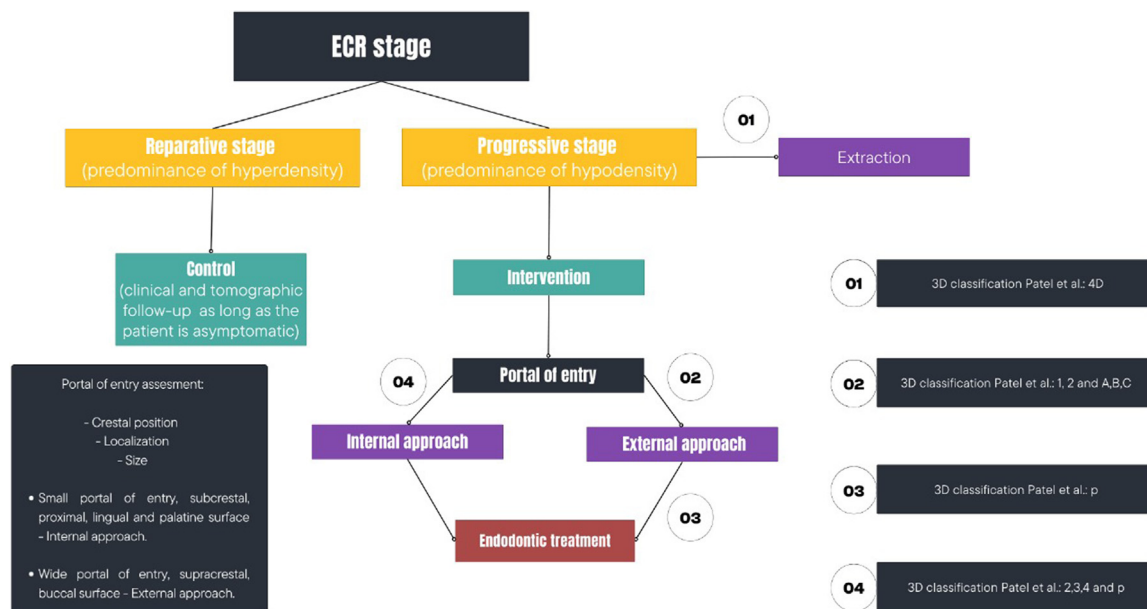
## REFERENCES

1. Rotondi O, Waldon P, Kim SG. The disease process, diagnosis and treatment of invasive cervical resorption: a review. *Dent J* 2020;8:1–12.
2. Patel S, Mavridou AM, Lambrechts P, et al. External cervical resorption-part 1: histopathology, distribution and presentation. *Int Endod J* 2018a;51:1205–23.
3. Patel K, Mannocci F, Patel S. The assessment and management of external cervical resorption with periapical radiographs and cone-beam computed tomography: a clinical study. *J Endod* 2016;42:1435–40.
4. Vaz de Souza D, Schirru E, Mannocci F, et al. External cervical resorption: a comparison of the diagnostic efficacy using 2 different cone-beam computed tomographic units and periapical radiographs. *J Endod* 2017;43:121–5.
5. Rodriguez G, Abella F, Durán-Sindreu F, et al. Influence of cone beam computed tomography in clinical decision making among specialists. *J Endod* 2017;43:194–9.
6. Mazón MR, Garcia-Font M, Doria G, et al. Influence of cone-beam computed tomography in clinical decision-making among different specialists in external cervical resorption lesions: a before-after study. *J Endod* 2022;48:1121–8.
7. AAE/AAOMR Joint Position Statement. Available at: <https://f3f142zs0k2w1kg84k5p9i1o-wpeengine.netdnassl.com/specialty/wpcontent/uploads/sites/2/2017/06/conebeamstatement.pdf>. [Accessed 19 February 2022].
8. Patel S, Lambrechts P, Shemesh H, Mavridou A. European Society of Endodontology position statement: external cervical resorption. *Int Endod J* 2018;51:1323–6.
9. Mavridou AM, Hauben E, Wevers M, et al. Understanding external cervical resorption in vital teeth. *J Endod* 2016;42:1737–51.



10. Heithersay GS. Invasive cervical resorption. *Endod Topics* 2004;7:73–92.
11. Shemesh A, Levin A, Hadad A, et al. CBCT analyses of advanced cervical resorption aid in selection of treatment modalities: a retrospective analysis. *Clin Oral Investig* 2018;23:1635–40.
12. Asgary S, Nourzadeh M, Verma P, et al. Vital pulp therapy as a conservative approach for management of invasive cervical root resorption: a case series. *J Endod* 2019;45:1161–7.
13. Patel S, Foshi F, Mannocci F, et al. External cervical resorption: a three dimensional classification. *Int Endod J* 2018b;51:206–14.
14. Patel S, Foshi F, Condon R, et al. External cervical resorption: part 2-management. *Int Endod J* 2018c;51:1224–38.
15. Espona J, Roig E, Durán-Sindreu F, et al. Invasive cervical resorption: clinical management in the anterior zone. *J Endod* 2018;44:1749–54.
16. Salzano S, Tirone F. Conservative nonsurgical treatment of class 4 invasive cervical resorption: a case series. *J Endod* 2015;41:1907–12.
17. Heithersay GS. Invasive cervical resorption: an analysis of potential predisposing factors. *Quintessence Int* 1999;30:83–95.
18. Mavridou A, Bergmans L, Barendregt D, et al. Descriptive analysis of factors associated with external cervical resorption. *J Endod* 2017;43:1602–10.
19. Patel S, Durack C, Abella F, et al. Cone beam tomography in endodontics-a review. *Int Endod J* 2021;54:18919–39.
20. Dias DR, Iwaki LCV, Oliveira ACA, et al. Accuracy of high resolution small-volume cone beam computed tomography in the diagnosis of vertical root fracture: an *In vivo* analysis. *J Endod* 2019;46:1059–66.
21. Pereira AMY, Pasqui DM, Amorim FC, et al. STROBE – checklist for reporting these observations. Students for Better Evidence. Cochrane. Available at: <https://eme.cochrane.org/strobe-checklist-para-relatar-estudos-observacionais>. [Accessed 20 November 2022].
22. Altman DG. *Practical Statistics for Medical Research*, 1. London: Chapman and Hall; 1991. p. 341–58.
23. Krippendorff K. *Content Analysis: An Introduction to its Methodology*, 3. Thousand Oaks, CA: Sage; 2004. p. 241–3.
24. IBM Corp. *IBM SPSS Statistics for Windows, Version 26.0*. Armonk, NY: IBM Corp; 2019.
25. Irinakis E, Aleksejuniene J, Shen Y, et al. External cervical resorption-a retrospective case control study. *J Endod* 2020;46:1420–7.
26. Ferreira MD, Costa-Barros M, Costa FF, et al. The prevalence and characteristics of external cervical resorption based on cone beam computed tomographic imaging: a cross-sectional study. *Restor Dent Endod* 2022;47:1–12.
27. Po-Yuan J, Li-Deh L, Shu-Hui C, et al. Invasive cervical resorption-distribution, potential predisposing factors, and clinical characteristics. *J Endod* 2020;46:475–82.
28. Mavridou AM, Pyka G, Kerckhofs G, et al. A novel multimodular methodology to investigate external cervical tooth resorption. *Int Endod J* 2016;49:287–300.
29. Consolaro A. External cervical resorption: diagnostic and treatment tips. *Dent Press J* 2016;21:19–25.
30. Carneiro ALE, Spin-Neto R, Zambrana NRM, et al. Quantitative and qualitative comparisons of pulp cavity volumes produced by cone beam computed tomography and micro-computed tomography through semiautomatic segmentation: an *ex vivo* investigation. *Oral Surg Oral Med Oral Pathol Oral Radiol* 2023;135:433–43.
31. Costa FF, Pinheiro LR, Umetsubo OS, et al. Influence of cone-beam computed tomographic scan mode for detection of horizontal root fracture. *J Endod* 2014;40:1472–6.
32. de Freitas JV, Baratto-Filho F, Coelho BS, et al. Efficacy of different cone-beam computed tomographic protocols in the identification of mesiobuccal canals of maxillary first molars: a tomographic and *ex vivo* study. *J Endod* 2017;43:810–5.
33. Wanderley VA, Neves FS, Nascimento MCC, et al. Detection of incomplete root fractures in endodontically treated teeth using different high-resolution cone-beam computed tomographic imaging protocols. *J Endod* 2017;43:1720–4.

## SUPPLEMENTARY MATERIAL



**SUPPLEMENTAL FIGURE S1** – Flowchart for endodontic treatment planning in external cervical resorption teeth, according to Patel et al classification<sup>2,13</sup>. 3D, 3-dimensional; 4D, 4-dimensional.